A combined theoretical and experimental determination of the electronic spectrum of acetone

Manuela Merchán
Departamento de Química Física, Universitat de València, Dr. Moliner 50, Burjassot, E-46100 Valencia, Spain

Björn O. Roos
Department of Theoretical Chemistry, Chemical Centre, P.O.B. 124, S-221 00 Lund, Sweden

Ruth McDiarmid and Xing Xing
Laboratory of Chemical Physics, National Institute of Diabetes and Digestive and Kidney Diseases, National Institutes of Health, Bethesda, Maryland 20892

(Received 23 August 1995; accepted 23 October 1995)

A combined *ab initio* and experimental investigation has been performed of the main features of the electronic spectrum of acetone. Vertical transition energies have been calculated from the ground to the $n_y \rightarrow \pi^*$, $\pi \rightarrow \pi^*$, $\sigma \rightarrow \pi^*$, and the $n=3$ Rydberg states. In addition, the $^1A_1$ energy surfaces have been studied as functions of the CO bond length. The $^1A_1$ $3p$ and $3d$ states were found to be heavily perturbed by the $\pi \rightarrow \pi^*$ state. Resonant multiphoton ionization and polarization-selected photoacoustic spectra of acetone have been measured and observed transitions were assigned on internal criteria. The calculated vertical transition energies to the $n_y \rightarrow \pi^*$ and all Rydberg states were found to be in agreement with experiment. This includes the $3s$-, all three $3p$-, and the A_1, B_1, and B_2 $3d$-Rydberg states. By contrast, there is little agreement between the calculated and experimental relative intensities of the A_1 and B_2 $3d$-Rydberg transitions. In addition, anomalously intense high vibrational overtone bands of one of the $3p$-Rydberg transitions have been observed. These results confirm the strong perturbation of the $3p$- and $3d$-Rydberg states by the $\pi \rightarrow \pi^*$ state found in the theoretical calculation and support the calculated position of this unobserved state. © *1996 American Institute of Physics.* [S0021-9606(96)00505-2]

I. INTRODUCTION

Acetone, the simplest aliphatic ketone, is probably the best experimentally studied molecule of this group of important organic systems. Because of the central position of acetone in many different areas of chemistry, the interpretation of its electronic spectrum has been and remains a subject of active experimental investigation.[1–16] In contrast, the theoretical studies of the electronic spectroscopy of carbonyl compounds have mainly focused on formaldehyde (see Ref. 17 and references cited therein). The dimethyl analog has been theoretically much less investigated, undoubtly due to the larger size of the molecule. To our knowledge, there exist only three previous *ab initio* studies, one at the CI level,[18] one using the random phase approximation (RPA),[19] and a recent study employing the equation-of-motion coupled cluster (EOM-CC) method.[20]

Qualitatively, the interpretation of the valence electronic transitions of the carbonyl chromophore as performed in classic textbooks (see, e.g., Refs. 21 and 22) invokes a bonding π orbital of CO, a nonbonding $2p_y$ orbital on oxygen (hereafter named n_y), and an antibonding π^* orbital between C and O. In the ground state, the order of the orbital energies is $\pi < n_y < \pi^*$. In the case of acetone (C_{2v} symmetry with the z axis along the C–O bond) the lowest energy electron promotion is from the highest occupied molecular orbital (HOMO), the b_2 nonbonding n_y orbital, to the b_1 antibonding π^* orbital resulting in the $^{1,3}A_2$ ($n_y \rightarrow \pi^*$) states. The $^{1,3}A_1$ ($\pi \rightarrow \pi^*$) states for the carbonyl group have traditionally been expected to appear at energies similar to those found for the corresponding states in ethylene.[1] For acetone, there has, however, not been enough experimental evidence to confirm this expectation. Little has changed since 1963 when it was stated that "... there seems to exist no great agreement in the literature about even the location of the $\pi \rightarrow \pi^*$ absorption for carbonyl!."[1] This represents one of the as yet unresolved key problems of small carbonyl compounds. Recent theoretical studies of the formaldehyde molecule have shown that the potential curves for the lower excited states of this symmetry involve heavy mixing of Rydberg and valence excited configurations resulting in a complex intensity distribution in the electronic spectrum.[17,23,24] We shall show here, in a combined theoretical and experimental investigation, that a similar situation obtains in acetone.

Optical[1] and electron-impact spectroscopies[2,4,6] have shown that acetone possesses a low intensity band with a maximum at approximately 4.4 eV, which has been identified as belonging to the lowest energy transition—from the ground state to the $^1A_2$ ($n_y \rightarrow \pi^*$) valence excited state. It is dipole symmetry forbidden, which explains the low intensity. The corresponding triplet state has also been studied and it is generally believed that the two states interact strongly.[25–27] Rydberg series converging to the lowest ionization limit show up next in the spectrum. The band visible in the absorption spectrum with an origin at 6.35 eV (see Ref. 14 and references therein) is due to a transition to the $^1B_2$ ($n_y \rightarrow 3s$)

Downloaded¬29¬Jan¬2010¬to¬147.156.182.23.¬Redistribution¬subject¬to¬AIP¬license¬or¬copyright;¬see¬http://jcp.aip.org/jcp/copyright.jsp

Rydberg state. That the $^1A_2$ ($n_y \rightarrow 3p_x$), $^1A_1$ ($n_y \rightarrow 3p$), and $^1B_2$ ($n_y \rightarrow 3p_z$) are located at 7.36, 7.41, and 7.45 eV was established in the work by McDiarmid and Sabljić.[7] Possible $n_y \rightarrow 3d$-Rydberg series have also been observed.[2] In addition, the region of the acetone spectrum above the first IP shows a number of broad features.[6]

Despite the considerable effort devoted to the study of the electronic spectrum of acetone, it has not been possible to locate unambiguously the $^1A_1$ ($\pi \rightarrow \pi^*$) state. However, two-photon photoacoustic spectroscopy gives evidence of a coupling between this state and the $^1A_1$ ($n_y \rightarrow 3p$) Rydberg state.[11] Similar evidence is obtained from 2 and 3 photon resonantly enhanced multiphoton ionization (REMPI) spectra of transitions to the $3p$-Rydberg states.[15]

The present work is a combined experimental and theoretical effort to analyze the main transitions in acetone in the energy region below the first ionization threshold. In the theoretical investigation special attention is given to the $\pi \rightarrow \pi^*$ state and its interaction with Rydberg states of the same symmetry. It will be shown that both the $3p$- and the $3d$-Rydberg states are heavily perturbed by this interaction, leading to a complex intensity distribution in the spectrum around 8 eV. The theoretical study used the complete active space (CAS) SCF method[28] in combination with a multiconfigurational second-order perturbation approach, the CASPT2 method.[29–31] Its validity in calculating the differential correlation effects on excitation energies has been demonstrated in a number of earlier applications.[32] Particularly relevant for the present work is the recent study of the electronic spectrum of formaldehyde, which included both the most prominent valence excited states together with a large number of Rydberg states. Both adiabatic and vertical transitions were studied.[17] In the experimental investigation polarization-selected photoacoustic (PA) and resonant multiphoton ionization (REMPI) spectroscopic measurements on static samples of acetone and acetone-d_6 and REMPI measurements on jet-cooled specimens were carried out to search for, and distinguish, long- and short-lived excited states. The new data were compared with the corresponding optical and electron-impact spectra of acetone. It will be shown that all discrete transitions occuring in the spectral region within about 0.2 of 7.9 eV are to perturbed vibrational sublevels of lower energy states. Previous assignments in this energy region are, consequently, incorrect. Higher energy transitions will also be shown to be perturbed, in full agreement with the theoretical results.

II. THEORETICAL METHODS AND COMPUTATIONAL DETAILS

A. Basis sets and geometry

As in previous theoretical studies,[18,19] the calculations of the vertical transition energies were performed for the equilibrium structure of the ground state experimentally determined by Nelson and Pierce.[33] The molecule possesses C_{2v} symmetry with the molecule in the yz plane and the z axis bisecting the CCC angle. The methyl groups are rotated such that each of them has one hydrogen atom in the OCCC plane located so that the distance between these two hydrogen atoms is maximized.

TABLE I. CASSCF wave functions (number of active electrons) employed to compute the valence and Rydberg transitions in acetone.

Wave function[a]	States	No. conf.[b]	N^c_{states}
CASSCF(2210)(6)	$^3A_2(n_y \rightarrow \pi^*)$	12	1
CASSCF(2210)(6)	$^3A_1(\pi \rightarrow \pi^*)$	9	1
CASSCF(2230)(6)	$^1A_1(n_y \rightarrow 3p_y, 3d_{yz}, \pi \rightarrow \pi^*)$	142	4
CASSCF(2200)(4)	$^1B_1(\sigma \rightarrow \pi^*)$	8	1
CASSCF(2211)(6)	$^1B_1(n_y \rightarrow 3d_{xy})$	43	1
CASSCF(6210)(6)	$^1B_2(n_y \rightarrow 3s, 3p_z, 3d_{x^2-y^2}, 3d_{z^2})$	516	4
CASSCF(2410)(6)	$^1A_2(n_y \rightarrow \pi^*, 3p_x, 3d_{xz})$	108	3

[a]Within parentheses the number of active orbitals of symmetry a_1, b_1, b_2, and a_2 of the point group C_{2v}.
[b]Number of configurations in the CASSCF wave function.
[c]States included in the average CASSCF calculation.

Generally contracted basis functions of the atomic natural orbital (ANO) type were used to construct the molecular orbitals.[34] The contraction scheme was C,O[$4s3p1d$]/H[$2s1p$], which has been shown in previous studies[35] to be flexible enough for a proper description of the valence excited states. Larger contracted sets were used in the previous study on formaldehyde to test the validity of this assumption.[17] Diffuse functions are required for the treatment of the $3s$, $3p$, and $3d$ Rydberg states. Using a recently developed procedure to obtain optimal Rydberg functions for a given system,[32] a final set of s-, p-, and d-type diffuse functions was built for acetone. The original basis set was supplemented with a $1s1p1d$ set of Rydberg functions (contracted from a set of $8s8p8d$ primitives), which was placed in the charge centroid of the $^2B_2$ state of the acetone cation. The C,O[$4s3p1d$]/H[$2s1p$]$+1s1p1d$ basis set was employed throughout.

B. CASSCF and CASSI calculations

Multiconfigurational wave functions were initially determined at the CASSCF level of approximation.[28] The carbon and oxygen $1s$ electrons were kept frozen in the form determined by the ground state SCF wave function. At the experimental geometry,[33] the total SCF energy for the ground state was calculated to be $-192.031\,706$ a.u. The choice of an active space for the CASSCF wave function is determined by the type of excited states to be studied. Here, they are the valence excited states and excitations to the $3s$, $3p$, and $3d$ Rydberg orbitals. In order to limit its size, different active spaces are used for different types of excited states. Experience shows that as long as the active space comprises the orbitals relevant for the excited states under consideration and is large enough that no intruder states appear in the CASPT2 calculations, the results are stable with respect to a further extension of the active space.[32] We shall label the active spaces ($klmn$), where the indices give the number of active orbitals in the four representations of the C_{2v} point group in the order a_1, b_1, b_2, and a_2. The active space used and the types of excited states computed are given in Table I.

Downloaded¬29¬Jan¬2010¬to¬147.156.182.23.¬Redistribution¬subject¬to¬AIP¬license¬or¬copyright;¬see¬http://jcp.aip.org/jcp/copyright.jsp

In addition to the vertical transitions, an attempt is made to analyze the behavior of the $^1A_1$ energy surfaces as functions of the CO distance (keeping all other geometry parameters fixed at their experimental values). This is done in order to get some insight into possible interactions between the valence and Rydberg excited states of this symmetry. The equilibrium CO bond length of the $^1A_1$ ($\pi\rightarrow\pi^*$) state is expected to be much longer than in the ground state. This will also affect the description of the CO σ bond and it becomes necessary to also allow for changes of the electronic structure in this bond in the CASSCF wave function. This is accomplished by making both the π,π^* and the σ,σ^* pairs of MOs active with four active electrons. Since some of the excited states correspond to excitation out of the in plane oxygen lone-pair orbital, n_y, the active space is further enlarged to (2210) with six active electrons. In order to avoid further complication, this active space was used throughout with the addition of appropriate Rydberg orbitals of the different symmetries. Details can be found in Table I. The valence and Rydberg excited states of $^1B_1$ symmetry were treated slightly differently: The actual choice of active space was (2200) and (2211), respectively. In this way it became possible to compute each state as the first root of the corresponding CASSCF wave function. For the valence excited states $^{1,3}A_1$ ($\pi\rightarrow\pi^*$) and $^1B_1$ ($\sigma\rightarrow\pi^*$), the HOMO $n_y(b_2)$ is inert with an occupation number close to two. The computed vertical transition energies for the valence excited states of these symmetries are therefore essentially independent of whether the oxygen lone-pair orbital is active or not (computed energies differ by less than 0.04 eV). The situation is different for the σ,σ^* pair. The effect of making the σ orbital active is non-negligible for states of A_1 symmetry, in particular for the $^1A_1$ ($\pi\rightarrow\pi^*$) state. This can be related to the correlation energy of the CO bond pair, which is larger in the ground state than in the excited state. Inclusion of the σ,σ^* pair into the active space increases the excitation energy to the $^1A_1$ ($\pi\rightarrow\pi^*$) state by 0.4 eV. This is more than expected and is not in accordance with the general behavior of the CASPT2 method. The result ought to be more stable with respect to this increase of the active space, at least for the vertical transition where the CO bond is short. For example, the corresponding effect in formaldehyde was only 0.1 eV.[17] Similar difficulties in using the approach to describe a $\pi\rightarrow\pi^*$ excited state in a double bond was also found for ethylene.[36] It seems that the coupling between the σ and π electrons is too strong to be treated fully with the perturbation approach. It should be added that the effect on the other states of A_1 symmetry is much smaller. In spite of this instability, we believe that the results obtained with the σ electrons active have the normal CASPT2 error bar of ± 0.3 eV.

The molecular orbitals for the excited states were obtained from average CASSCF calculations, where the averaging includes all states of interest for a given symmetry. The number of such states is also listed in Table I together with the number of configuration functions (CFs) in the CASSCF wave function. Transition moments were computed at the CASSCF level of theory using the CAS state interaction method.[37] Earlier experience has shown that these quantities can be accurately computed at this level of theory, since they are less affected by dynamical correlation energy than the energies.

C. The CASPT2 method

The CASPT2 method[29–31] computes the first-order wave function and the second-order energy in the full CI space with a CASSCF wave function constituting the reference function. The full Fock matrix in the definition of the zeroth-order Hamiltonian was used.[30] The weight of the CASSCF reference in the first-order wave function was found to be within the range 0.82–0.85 in all cases (with the exception of the $\pi\rightarrow\pi^*$ state, where it is somewhat lower). This weight is a measure of how a large fraction of the wave function is treated variationally. Normally a balanced calculation with respect to the treatment of electron correlation yields about the same weight for the ground and the excited states.

The calculations were performed on the IBM 9021/500-2VF computer of the University of Valencia using the MOLCAS-3 quantum chemistry software.[38]

III. EXPERIMENTAL METHODS

The experimental details have been published previously.[15] Briefly, jet-cooled (3+1) resonant multiphoton ionization (REMPI) spectra were measured on a conventional supersonic molecular beam coupled with a time of flight (TOF) mass spectrometer. It was not possible to measure the (2+1) REMPI spectrum because of interference by (1+2) resonances. The molecular beam was obtained by expanding 3 atm Ar seeded with 30 Torr acetone or acetone-d_6 through a pulsed 500 μm nozzle into a chamber pumped by two turbomolecular pumps. ''Warmer'' samples were generated either by increasing the sample pressure to 60 Torr or by reducing the backing pressure to 1 atm. The ions were mass resolved but the spectrum of the region studied here was mass independent.

Simultaneous REMPI and photoacoustic (PA) spectra were measured on static samples of acetone, as was done previously,[39] however the REMPI spectra so obtained were extremely power broadened. Additional spectra were measured with much lower laser power; these spectra will be presented here. In both cases a biased electrode was placed inside the PA cell for ion collection. PA signals were detected by a condenser microphone (Knowles model BT-1759). REMPI spectra were measured on approximately 2 Torr samples of acetone. PA measurements were made on 30 Torr samples.

The laser system was a conventional injection-seeded Quanta-Ray YAG pumped dye system. Circular or linear polarization of the laser light was produced by a double- and single-Fresnel rhomb arrangement. Since the main results desired from this experiment were the positions of the bands and the relative intensities of closely spaced transitions, the spectra were not normalized for the wavelength dependence of the light intensity. Commercial acetone and acetone-d_6 were vacuum distilled when used. Chromatographic grade argon was used as supplied.

Downloaded¬29¬Jan¬2010¬to¬147.156.182.23.¬Redistribution¬subject¬to¬AIP¬license¬or¬copyright;¬see¬http://jcp.aip.org/jcp/copyright.jsp

IV. THEORETICAL RESULTS AND ANALYSIS

The numerical results obtained in the calculations will be presented and discussed in this section. Of primary interest is the study of the interaction between Rydberg and valence excited states. This can only be fully achieved with access to the full energy hypersurfaces, an obviously difficult task. We have not attempted to perform such a study. However, one degree of freedom along which the energy of the $^1A_1$ ($\pi \rightarrow \pi^*$) excited state can be expected to vary strongly is the CO distance. The CO stretching potentials have therefore been computed for the electronic states of $^1A_1$ symmetry with all other degrees of freedom fixed at the experimental equilibrium values. In addition to this detailed study of the $^1A_1$ states, vertical excitation energies will be presented for a large number of states.

A. Potential curves for the $^1A_1$ states

One of the main features expected for the equilibrium geometry of the $^1A_1$ ($\pi \rightarrow \pi^*$) excited state is a considerably increased CO distance compared to the ground state, since the excitation is from a bonding to an antibonding orbital. We have computed the energy as a function of the CO bond length for the four lowest electronic states of $^1A_1$ symmetry (the ground state, the $\pi \rightarrow \pi^*$ state, and the $n_y \rightarrow 3p$ and $n_y \rightarrow 3d$ Rydberg states). Such a calculation is not straightforward with the present theoretical approach because of the interaction between Rydberg and valence excited states. The reference functions for the perturbation calculation of the correlation energy are determined at the CASSCF level of approximation. However, at this level the interaction between the different states can be in error, since the dynamic correlation effects are normally larger for valence excited states than for Rydberg states. In the region of the crossing, the reference functions will not correctly describe the mixing of the different states. This error cannot be corrected by a second order treatment, since higher order terms that mix the different reference functions are needed. Only a multistate theory, which includes this mixing in the perturbation treatment, can solve this problem. The problem does not arise for the vertical transitions in acetone, since there is no Rydberg–valence mixing at the ground state equilibrium geometry. In other systems, however, this problem has led to increased errors in some $\pi \rightarrow \pi^*$ excitation energies (see, for example, the results for ethene and butadiene in Ref. 36).

The interaction between Rydberg and valence excited states can be assumed to be weak and therefore only important close to the crossing points for the corresponding potential curves. One solution is to neglect the coupling by performing the calculations in such a way that the two types of states do not appear together. This approach has been used here to calculate the potential curves for the $^1A_1$ excited states. For CO distances shorter than 1.5 Å, $\pi \rightarrow \pi^*$ is the fourth excited state at the CASSCF level. Calculations with the active space (2230) and six active electrons were performed in this region. The CASSCF state average calculation included three roots (the ground state, the $n_y \rightarrow 3p$ and the $n_y \rightarrow 3d$ states). The $3p_x$ and $3d_{xz}$ orbitals were deleted from the MO space in order to avoid intruder state problems from excitations to these orbitals from the occupied π orbital. The $\pi \rightarrow \pi^*$ excited state potential was obtained with the active space (2200), which does not include the n_y and the Rydberg orbitals. Only the four electrons of the CO bond were active. The two Rydberg orbitals of π symmetry, $3p_x$ and $3d_{xz}$, were deleted as before. Two results give an indication of the stability of the approach. First, the two potential curves for the ground state were virtually identical. Second, the computed vertical excitation energy for the $\pi \rightarrow \pi^*$ state was 9.20 eV, which is only 0.04 eV larger than the value obtained with the larger active space. The latter was used for all the vertical transitions (cf. Tables I and III). This illustrates again that the CASPT2 results are stable with respect to modifications in the active space, as long as they do not grossly change the structure of the CASSCF reference function.

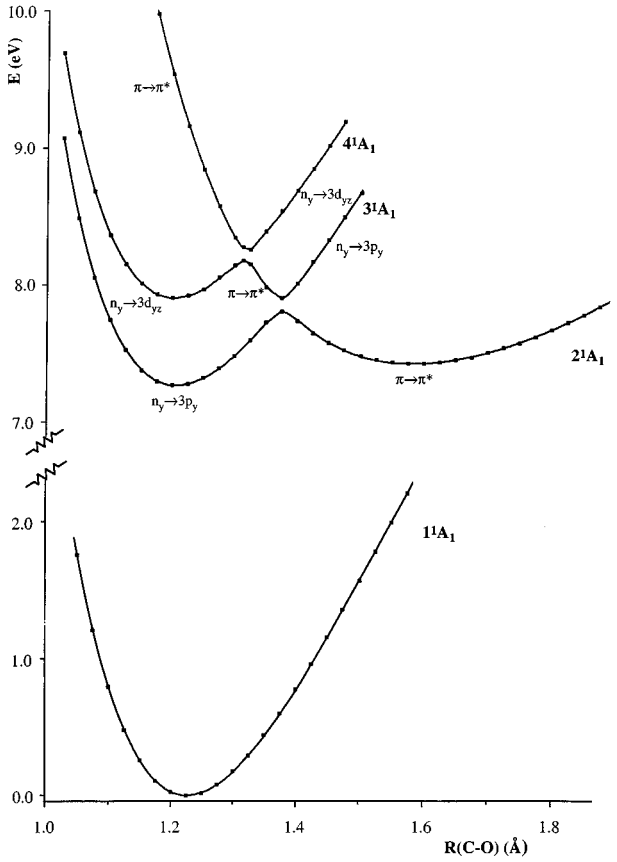

FIG. 1. Potential curves for the $^1A_1$ states as a function of the CO bond length. The avoided crossings have been made by hand. Data for the stationary points can be found in Table II, which also includes a vibrational analysis.

The resulting potential curves are shown in Fig. 1. The computed curves cross each other, but in the figure the avoided crossings have been indicated by introducing a small separation. The minimum of the ground state curve is found for $r(\mathrm{CO})=1.226$ Å with $\nu_3(\mathrm{CO})=1698$ cm^{-1}, which compares favorably to the experimental results, 1.222 Å, 1731 cm^{-1}.[15,33] The 2 $^1A_1$ state has a double minimum potential. The inner minimum is dominated by the $3p_y$ Rydberg state

Downloaded¬29¬Jan¬2010¬to¬147.156.182.23.¬Redistribution¬subject¬to¬AIP¬license¬or¬copyright;¬see¬http://jcp.aip.org/jcp/copyright.jsp

with an equilibrium bond length slightly shorter than that of the ground state. The outer minimum is the $\pi\rightarrow\pi^*$ state. It is located 7.42 eV above the ground state at a CO distance of 1.58 Å. The excitation energy has thus decreased 1.78 eV compared to the vertical value.

In order to check the influence of the remaining geometry parameters on the computed T_e value, the r(CO), r(CC) distances and the CCC angle were optimized for both the ground state and the $^1A_1$ ($\pi\rightarrow\pi^*$) valence excited state at the CASPT2 level [active space (2200) with four active electrons]. The geometry of the CH_3 group was kept fixed at the values obtained for the ground state by a full geometry optimization at the CASSCF level. The optimized CO (1.222 Å) and CC (1.510 Å) distances, as well as the CCC angle (116.0°) for the ground state agree with experiment (1.222 Å, 1.507 Å, and 117.2°[33]). The CO distance in the excited state increased to 1.601 Å, which is close to the location of the outer minimum on the potential curve of the second $^1A_1$ state as shown in Fig. 1. The optimal CC distance, 1.456 Å, is 0.054 Å shorter than it is in the ground state. This is a surprising change, indicating an enhanced coupling between the π system and the CH_3 groups. The bond angle opens up to 127.3°, as is expected due to the radical character of the $C(CH_3)_2$ group. The computed T_e value is 7.19 eV.

The third $^1A_1$ state has also a double minimum potential along the C═O stretch coordinate. It contains contributions from all three diabatic curves. The inner minimum is dominated by the $3d_{yz}$-Rydberg state, while the outer minimum arises from the avoided crossing between the $\pi\rightarrow\pi^*$ and the $3p_y$ states. The apparent fourth $^1A_1$ state is a combination of the wings of the $\pi\rightarrow\pi^*$ state and the $3d_{yz}$ state. However, as the inner potential of this state will cross that of the $^1A_1$ $4p$-Rydberg state, which was not calculated here, it too will have a double minimum potential along this coordinate. The calculated sharp minimum at 1.32 Å, 8.26 eV above the ground state is the outer minimum of this fourth $^1A_1$ state. More data for the potential curves are given in Table II.

We also calculated the electronic transition moments for excitation from the ground state to the three $^1A_1$ states studied here as functions of the CO distance. All three transition moments vary smoothly with CO distance. For the diabatic $3p_y$-Rydberg state the values vary from about 0.11 at short distances to 0.00 at r(CO)=1.5 Å. The corresponding values for the $3d_{yz}$-Rydberg state are 0.59 to 0.45, and for the $\pi\rightarrow\pi^*$ state 1.26 to 0.75 [at r(CO)=1.95 Å]. We used these data to perform a vibronic analysis, treating the system as a diatomic molecule. This is obviously a crude approximation, since it neglects all couplings to other modes and only treats the CO stretch frequency. Nevertheless, such a study might give some insight into the intensity distribution for excitations from the ground state to the three excited states. Note that this calculation neglects all vibronic coupling between the three excited states. We have therefore only considered the lowest vibrational quantum numbers of each state. Within this crude model the calculation is exact. The numerical Schrödinger equation has been solved and the intensities have been computed by numerical integration of the transition dipole matrix elements for the different vibrational wave functions (the VIBROT program of the MOLCAS package was used). Only excitations out of the $v''=0$ ground state level have been considered.

TABLE II. Vibrational analysis (for the $0\rightarrow v'$ transitions) and other spectroscopic results for the computed potential curves of $^1A_1$ excited states in acetone (cf. Fig. 1).

State	r_e(Å)	T_e(eV)	v'	ΔE(eV)	f[a]
$1\,^1A_1$					
Minimum	1.226	0.00	0	0.11	
$2\,^1A_1$					
Inner min.	1.205	7.26	0	7.25	$8.4\cdot10^{-4}$
Maximum	1.375	7.81	1	7.36	$3.8\cdot10^{-8}$
Outer min.	1.584	7.42	2	7.54	$2.2\cdot10^{-6}$
			3	7.62	$1.4\cdot10^{-5}$
			4	7.64	$1.1\cdot10^{-6}$
			5	7.72	$3.8\cdot10^{-6}$
$3\,^1A_1$					
Inner min.	1.202	7.90	0	7.89	0.0414
Maximum	1.314	8.18	1	7.97	0.0032
Outer min.	1.373	7.90	2	8.10	0.0022
$4\,^1A_1$					
Minimum	1.321	8.26	0	8.35	0.0178
			1	8.68	0.0560
			2	8.93	0.0777

[a]Calculated oscillator strength.

The results are given in Table II. They show that the CO stretch vibrational subbands of the $2\,^1A_1$ system should be weak. The largest intensity is obtained for the 0–0 transition at 7.25 eV. The two lowest vibrational subbands ($v=0,1$) are entirely confined to the Rydberg part of the potential. It is only the third subband ($v=2$) that has any contribution from the $\pi\rightarrow\pi^*$ potential. But here the Franck–Condon overlap between the ground state and the $\pi\rightarrow\pi^*$ state is small. The largest intensity for bands below 8.0 eV is found for the 0–0 transition to the $3\,^1A_1$ state, which occurs at 7.9 eV. This is the $n_y\rightarrow3d_{yz}$ transition. Appreciable intensity contributions from the $\pi\rightarrow\pi^*$ excited state appear only for the $4\,^1A_1$ potential and start at 8.35 eV, although with the inclusion of higher Rydberg states omitted from the calculation this intensity is likely to be further diluted. These results will be compared with the observations in the discussion.

Recent theoretical studies of formaldehyde by Hachey *et al.*[24] and by the present authors[17] have revealed more features of the potential surfaces. The similarity between formaldehyde and acetone makes it possible to draw conclusions for the latter molecule based on the results obtained for formaldehyde, especially since the results obtained here for the $^1A_1$ states of acetone are similar in quality to those obtained by Hachey *et al.* In formaldehyde the $^1B_1$ ($\sigma\rightarrow\pi^*$) potential has a minimum at r(CO)=1.47 Å and crosses the $^1A_1$ ($\pi\rightarrow\pi^*$) surface close to this point. Bending the CH_2 group out of plane causes the two states to mix. The optimum bending angle for the lower component of the mixed states, predominantly the $\sigma\rightarrow\pi^*$ component, was computed to be 46°. At shorter distances the $^1B_1$ surface mixes strongly with the $^1B_1$ ($n_y\rightarrow3d_{xy}$) state. It is likely that a similar situation ob-

Downloaded¬29¬Jan¬2010¬to¬147.156.182.23.¬Redistribution¬subject¬to¬AIP¬license¬or¬copyright;¬see¬http://jcp.aip.org/jcp/copyright.jsp

TABLE III. Calculated and experimental excitation energies (in eV) and other properties of the vertical excited states of acetone.

State	CASSCF	CASPT2	Current Expt.	Other Expt.	μ[a]	Total[b] $\langle x^2\rangle$	Total[b] $\langle y^2\rangle$	Total[b] $\langle z^2\rangle$	Osc. Str.	Other results CI[c]	Other results RPA[d]	Other results EOM-CC[e]
Ground state ($1\,^1A_1$)					−1.151	17.9	17.8	21.3				
Singlet states												
$1\,^1A_2(n_y\rightarrow\pi^*)$	5.72	4.18		4.38[f]	−0.895	18.7	15.0	18.6	Forbidden	4.41	3.33	4.48
$1\,^1B_2(n_y\rightarrow 3s)$	6.39	6.58		6.35[g]	+0.192	43.7	31.7	36.1	0.0152	6.20	6.89	6.39
$2\,^1A_1(n_y\rightarrow 3p_y)$	7.01	7.26		7.41[h]	−0.451	37.5	74.0	35.7	0.0001	7.32	7.76	7.45
$2\,^1A_2(n_y\rightarrow 3p_x)$	7.44	7.34		7.36[h]	−0.410	69.7	30.6	32.1	Forbidden	7.01	7.58	7.41
$2\,^1B_2(n_y\rightarrow 3p_z)$	7.10	7.48		7.45[h]	+0.455	36.0	31.5	74.2	0.0017	7.17	7.71	7.51
$3\,^1A_1(n_y\rightarrow 3d_{yz})$	7.55	7.91	7.8		+1.097	38.0	78.1	81.0	0.0431		8.37	8.23
$3\,^1B_2(n_y\rightarrow 3d_{x^2-y^2})$	7.62	8.04	8.09		−0.123	71.3	68.2	42.5	0.0065	7.91	8.26	7.95
$3\,^1A_2(n_y\rightarrow 3d_{xz})$	8.13	8.09			+1.034	78.3	33.9	77.9	Forbidden		8.38	8.44
$4\,^1B_2(n_y\rightarrow 3d_{z^2})$	7.72	8.18			−0.534	41.5	65.2	88.4	$8\cdot10^{-5}$		8.39	8.48
$1\,^1B_1(n_y\rightarrow 3d_{xy})$	7.49	8.20	8.17		−0.026	81.6	77.0	36.1	0.0023		8.41	8.43
$2\,^1B_1(\sigma\rightarrow\pi^*)$	10.37	9.10			−0.388	18.9	18.4	19.0	0.0095		8.15	9.30
$4\,^1A_1(\pi\rightarrow\pi^*)$	10.70	9.16			−1.551	17.5	16.1	21.3	0.3263	11.30	8.63	9.15
Triplet states												
$1\,^3A_2(n_y\rightarrow\pi^*)$	4.55	3.90		4.16[i]	−0.449	19.0	17.8	19.9		4.04		
$1\,^3A_1(\pi\rightarrow\pi^*)$	6.27	5.98		5.88[i]	−0.437	18.1	18.9	20.6		5.73		

[a]Dipole moment (CASSCF) in a.u. (experimental value for the ground state is 1.14 a.u. [J. D. Swalen and C. C. Costain, J. Chem. Phys. **31**, 1562 (1959)].
[b]Expectation value (CASSCF) of x^2, y^2, and z^2 (in a.u.).
[c]CI results from Ref. 18.
[d]RPA results from Ref. 19.
[e]EOM-CC results from Ref. 20.
[f]Electron-impact data from Ref. 6.
[g]See Ref. 14 and references therein.
[h]RMPI data from Ref. 7.
[i]Electron-impact data from Refs. 4 and 6.

tains in acetone. Thus in acetone the CO stretch is expected to allow the mixing of the $^1B_1$ ($\sigma\rightarrow\pi^*$) and the $^1B_1$ ($n_y\rightarrow 3d_{xy}$) states while out of plane modes in combination with the CO stretch will allow the mixing of the valence $^1A_1$ and $^1B_1$ states. This will further complicate the vibrational spectrum, compared to the simplified analysis performed above.

In addition, the bent $2\,^1A'$ ($\sigma\rightarrow\pi^*,\pi\rightarrow\pi^*$) can be expected to couple with the $^1B_2$ ($n_y\rightarrow 3s$) state through the antisymmetric a'' modes, as they have been shown to do in formaldehyde.[23] The equilibrium geometry for the $^1A_2$ ($n_y\rightarrow\pi^*$) state is likewise expected to be bent (in formaldehyde the bending angle is calculated to be 31°[17]). The results obtained by Hachey *et al.* for H_2CO show that the $2\,^1A_2$ ($n_y\rightarrow 3p_x$) potential is also crossed by the $^1B_1$ ($\sigma\rightarrow\pi^*$) potential. Thus the dipole forbidden transition to the $^1A_2$ state can become vibrationally allowed, borrowing intensity from the interfering $^1B_1$ state via modes of b_2 symmetry.

Assuming the two molecules to be similar, we conclude that all the $n_y\rightarrow$Rydberg states may mix through vibronic interactions with the valence excited states of $^1A_1$ and $^1B_1$ symmetry. The large transition moment of the $^1A_1$ ($\pi\rightarrow\pi^*$) state can consequently be used to give intensity to Rydberg states of $^1A_1$, $^1B_1$, and $^1B_2$ symmetry. Direct configurational mixing is also a possible mechanism for states of the same symmetry. A direct observation of the $\pi\rightarrow\pi^*$ state is, on the other hand, predicted to be difficult due to the small Franck–Condon factors for the lower vibrational levels.

B. Vertical transition energies

In addition to the detailed study of the $^1A_1$ states, we have calculated the vertical transition energies for a number of valence excited states and for excitations to the $3s$, $3p$, and $3d$ Rydberg states from the n_y orbital. The calculations were performed at the experimental geometry[33] using the active space given in Table I. At this geometry there is no near degeneracy between the Rydberg and valence excited states, so the CASSCF solutions are valid reference functions for the perturbation treatment. The results are therefore expected to have the normal error bars of the present approach: ±0.3 eV. This is a conservative estimate and we expect, based on previous experience, that the accuracy of most results will be well below this limit.

The results are presented in Table III. The first column in this table identifies the different excited states. The second and third column give the vertical transition energies (in eV) as obtained by the CASSCF and CASPT2 method, respectively. The CASSCF energies are presented in order to show how large the dynamical correlation is for the different excited states. Normally, the effect is to raise the energies of the Rydberg states (more correlation in the ground state) and lower those of the valence states, hence to decrease the calculated transition energies. As can be seen in the table, this rule is fulfilled with the exception of the Rydberg states of $^1A_2$ symmetry. We have not tried to analyze this deviation from the rule in detail. Column four contains the experimental transition energies obtained in the current study, which

Downloaded¬29¬Jan¬2010¬to¬147.156.182.23.¬Redistribution¬subject¬to¬AIP¬license¬or¬copyright;¬see¬http://jcp.aip.org/jcp/copyright.jsp

have been correlated with their corresponding calculated energies by symmetry and transition type. Other experimental data are given in column five. In the remainder of this table, μ is the dipole moment (in a.u.) computed at the CASSCF level and $\langle x^2\rangle$, $\langle y^2\rangle$, and $\langle z^2\rangle$ are the expectation values (in a.u.) of x^2, y^2, and z^2, respectively. By comparison with the ground state values it is straightforward to use these numbers to identify the Rydberg character of a given excited state. As the results show, there is almost no mixing between the two types of transitions. Computed oscillator strengths are given in column 10. They have been computed using transition moments obtained at the CASSCF level in combination with CASPT2 excitation energies, a method which has proven to work well in a number of earlier applications. *Ab initio* energies obtained in earlier studies are listed in columns 11–13.

1. Valence excited singlet states ($1\,^1A_2$, $2\,^1B_1$, and $4\,^1A_1$)

The lowest singlet state is of $^1A_2$ symmetry. The vertical excitation energy, computed at the CASPT2 level, 4.18 eV, is about 0.2 eV lower than the experimental estimates.[3,4,6] The lowest singlet band in the electron-impact spectrum reported by Walzl *et al.*[6] was assigned to the $^1A_2$ ($n_y\rightarrow\pi^*$) transition. It has an onset at 3.75 eV and a maximum at 4.38 eV. The measured intensity is low. In formaldehyde we optimized the geometry of this state as well as that of the ground state and a number of other excited states. The energy difference between the adiabatic and vertical transition energy was found to be 0.54 eV. If we use this value to estimate the adiabatic transition energy in acetone, we arrive at the value 3.64 eV, which is comparable to the onset of the band at 3.75 eV.

Previous theoretical studies also predict the lowest singlet excited state in acetone to be $^1A_2$. The early CI study by Hess *et al.* gave a value of 4.41 eV for the vertical energy.[18] The random phase approximation (RPA) underestimates the transition energy by about 1 eV,[19] even though an attempt was made to improve the results by replacing the valence–hole energies by the experimental ionization potentials. The recent EOM-CC calculations by Gwaltney and Bartlett gives on the other hand an excitation energy in agreement with experiment.[20] Calculations of the solvatochromic shifts have been performed using MCSCF theory with a reaction field Hamiltonian,[40] and by Monte Carlo simulations.[41]

The second valence excited state is $2\,^1B_1$ and is located 9.10 eV above the ground state. The computed intensity of the transition is 0.01. This state arises from an excitation out of the highest occupied σ orbital, of a_1 symmetry, to π^* ($\sigma\rightarrow\pi^*$). It has not been experimentally observed. As shown in the formaldehyde study, this state will mix with the $^1A_1$ ($\pi\rightarrow\pi^*$) state via a bending motion to form a $^1A'$ state with an adiabatic energy 1.66 eV lower than the vertical value. The vertical value in acetone is almost the same as in formaldehyde (9.09 eV). The RPA method places this state about 1 eV too low,[19] while the EOM-CC study gives it as the third valence excited state at 9.30 eV.[20]

The third valence excited state is $4\,^1A_1$ with a vertical excitation energy of 9.16 eV, 0.5 eV below the first ionization limit. The computed intensity is 0.33. This is the expected ($\pi\rightarrow\pi^*$) state. At the ground state geometry this state does not mix with other states. As discussed above, at other geometries such mixing occurs. Early CI studies placed this transition at 11.3 eV,[18] the RPA result is 8.63 eV.[19] A comparison of the transition energies for the valence excited states in acetone and formaldehyde[17] shows that this state changes its energy much more than the $^1A_2$ and the $^1B_1$ states: The calculated vertical transition energy for $^1A_1$ in formaldehyde is 9.77 eV, 0.61 eV above its energy in acetone. Also, the energy minimum in formaldehyde is 7.84 eV above the ground state while in acetone it is 7.42 eV. A possible explanation is the ionic character of the excited state, which is stabilized by the presence of the more polarizable methyl groups in acetone. The CASPT2 and EOM-CC results for the vertical energy are identical, which increases the confidence in the theoretical value for this unobserved electronic state.

2. Rydberg excited states

The first and second ionization potentials of acetone are separated by $\approx$3 eV.[13] The corresponding members of the Rydberg series converging on these ionization limits will, therefore, be separated by $\approx$3 eV. The results of the present study estimates the term value (IP—transition energy) of the first member of the ns Rydberg series to be in the range, 3.1–3.5 eV. Thus the first member of the ns Rydberg series to the second limit is estimated to lie close to the first ionization limit. We, therefore, limit the present study to the lower members of the first series, corresponding to excitation out of the n_y (HOMO) orbital to the $3s$ and the different components of the $3p$ and $3d$ Rydberg orbitals.

$n_y\rightarrow 3s$ ($1\,^1B_2$). The computed vertical excitation energy for this state is 6.58 eV. As previously reported, the origin of the $3s$ band is well established and appears at 6.35 eV. The calculations thus overestimates the excitation energy by 0.23 eV. A similar error was found in the recent study of formaldehyde.[17] This is exceptional, since earlier studies of Rydberg states give only small errors for the $3s$ state (less than 0.1 eV[32]). We have no explanation why this system behaves differently. A test calculation was performed with an uncontracted set of eight diffuse s-type primitive Gaussians, but the result was unchanged (6.53 eV). The EOM-CC results is in better agreement with experiment, indicating that the present error is due to the CASPT2 approximation rather than the basis set.

$n_y\rightarrow 3p$ ($2\,^1A_1$, $2\,^1A_2$, and $2\,^1B_2$). The computed values for the $2\,^1A_2$ ($n_y\rightarrow 3p_x$), 7.34 eV, and $2\,^1B_2$ ($n_y\rightarrow 3p_z$), 7.48 eV above the ground state, agree with measured transition energies,[7] 7.36 and 7.45 eV, respectively. The transition energies to the $2\,^1A_1$ ($n_y\rightarrow 3p_y$) state is, on the other hand, computed at 7.26 eV, 0.15 eV below the experimental value, 7.41 eV.[7] This error is related to the problems with the second order approach for states of the same symmetry as the $^1A_1$ ($\pi\rightarrow\pi^*$) state, as discussed above. But the error is acceptable and the CASPT2 results are consistent with experiment, both in excitation energy and assignment. It may be

Downloaded¬29¬Jan¬2010¬to¬147.156.182.23.¬Redistribution¬subject¬to¬AIP¬license¬or¬copyright;¬see¬http://jcp.aip.org/jcp/copyright.jsp

noted that transitions to both dipole allowed $3p$ states are calculated to have considerably smaller intensities than to the $3s$ state and that the transition to the $^1B_1$ state is calculated to be more than 10 times as intense as the transition to the $^1A_1$ state (cf. Table III). Both of these results are in agreement with the experimental observations.[5] The computed energies at the CI and EOM-CC levels are consistent with the present results.[18,20] The RPA results show larger deviations.[19]

$n_y \rightarrow 3d$ ($3\,^1A_1$, $3\,^1B_2$, $3\,^1A_2$, $4\,^1B_2$, and $1\,^1B_1$). The five members of the $3d$ series were computed to lie in the energy range 7.91–8.20 eV. The $3\,^1A_1$ ($n_y \rightarrow 3d_{yz}$) transition is calculated to be approximately seven times as intense as the next most intense ($n_y \rightarrow 3d$) transition, to the $3\,^1B_2$ state, and almost three times as intense as the ($n_y \rightarrow 3s$) transition. While the calculated transition energy to $3\,^1B_2$ agrees well with the transition energy of the one intense transition reported in this energy range, at 8.1 eV[5] the intensity correlation indicates that the optically observed transition is to $2\,^1A_1$. The analysis and assignment of this spectral range will be discussed after the experimental results have been analyzed.

3. Valence excited triplet states ($1\,^3A_2$,$1\,^3A_1$)

The two lowest triplet excited states were also included in the calculations. The $1\,^3A_2$ and $1\,^3A_1$ states were computed to lie 3.90 and 5.98 eV above the ground state, in agreement with experimental evidence.[4,6] The low-energy electron impact study of John *et al.* located the first triplet state at 4.16 eV and a very broad triplet feature ranging from 5.3 to 6.1 eV with an intensity maximum at 5.88 eV.[4] Scattering experiments performed by Walzl *et al.* also showed these bands.[6] The discrepancies between the computed and experimental data are within the experimental error bars. The earlier CI results also support these assignments.[18]

V. EXPERIMENTAL RESULTS AND ANALYSIS

The (3+1) REMPI spectra of jet-cooled acetone and acetone-d_6 from experimental wavelengths of 485 to 445 nm obtained with linearly polarized excitation are presented in Fig. 2. In general, the REMPI technique mainly detects transitions to Rydberg states because of their relatively long lifetimes and good Franck–Condon overlaps with the ion. The red ends of the spectra presented here overlap those previously published.[15] The intense bands of the two isotopomers in the blue region of the spectra are similar, as is usual for isotopomers. Surprisingly, the weaker bands in the red region of the spectra of the two isotopomers are dissimilar. Corresponding spectra obtained with circularly polarized excitation were measured. For three-photon resonances the ratio of the signal intensities for circularly/linearly polarized excitation is 5/2 for transitions of A_2 symmetry and less than 5/2 for all others.[42] In the $3p$-Rydberg$\leftarrow\tilde{X}$ system, the intensity of the (3+1) REMPI $^1A_1$ bands excited by circularly polarized light is less than 10% of that obtained with linearly polarized excitation.[15] The polarization-selected acetone spectra are presented in Fig. 3. All bands except a few very weak bands in the far blue are seen to be greatly decreased in intensity with circularly polarized excitation. We conclude that none of the bands observed here can be A_2. Because the spectra differ to the red and blue of 8 eV, the two spectral regions will be analyzed separately.

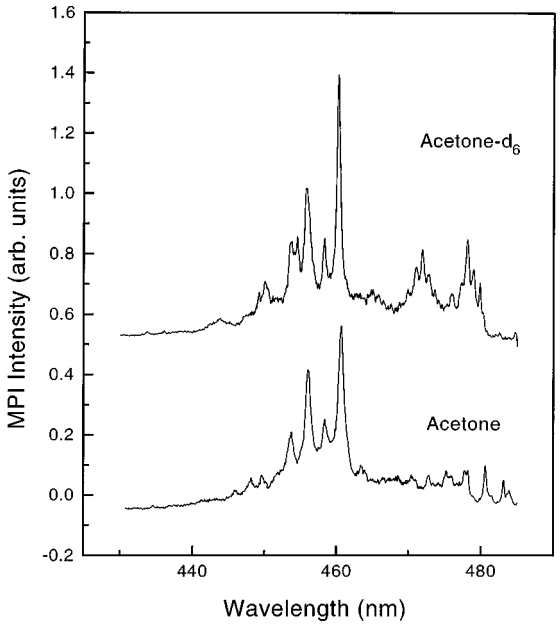

FIG. 2. Survey (3+1)REMPI spectra of jet-cooled acetone and acetone-d_6 excited with linearly polarized light. The deuteroacetone spectrum has been displaced upwards for clarity.

A. The 62 000–64 800 cm^{-1} (7.7–8.0 eV) spectral region

The (3+1) REMPI spectrum of jet-cooled acetone between 40 800 and 78 700 cm^{-1} has been presented above.

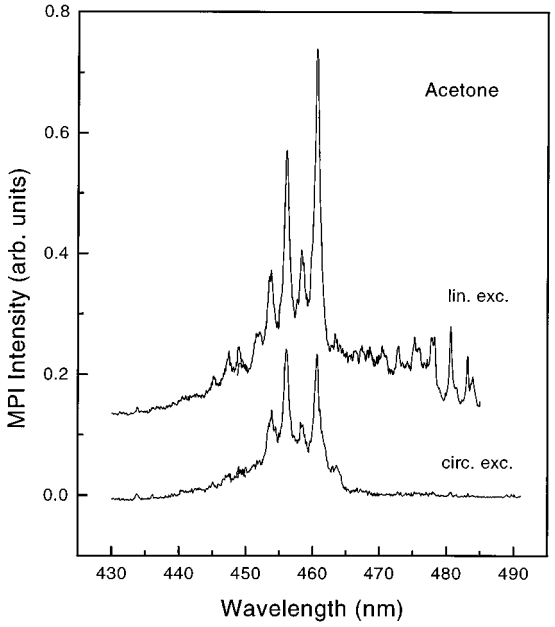

FIG. 3. (3+1)REMPI spectra of jet-cooled acetone excited with linearly and circularly polarized light. The spectrum obtained with linearly polarized excitation has been displaced upwards for clarity.

Downloaded¬29¬Jan¬2010¬to¬147.156.182.23.¬Redistribution¬subject¬to¬AIP¬license¬or¬copyright;¬see¬http://jcp.aip.org/jcp/copyright.jsp

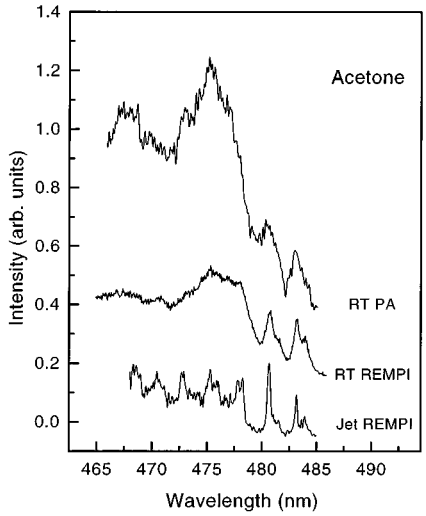

FIG. 4. (3+1) Jet-cooled and room temperature REMPI spectra and the (RT) photoacoustic spectrum of acetone. The three spectra been displaced for clarity. The relative intensities of the three spectra have been scaled to agree between 480 and 485 nm.

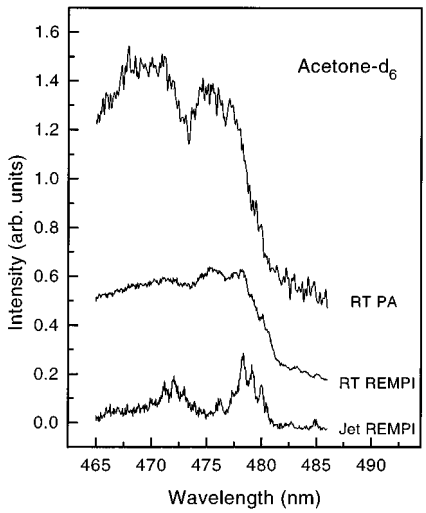

FIG. 5. (3+1) Jet-cooled and room temperature REMPI spectra and the (RT) photoacoustic spectrum of deuteroacetone. The three spectra have been displaced for clarity. The relative intensities of the three spectra have been scaled as for Fig. 4.

The corresponding optical (i.e., one-photon) absorption spectrum has been recorded at room temperature.[5] The REMPI spectrum of acetone is similar to the optical spectrum between 62 000 and 62 500 cm^{-1} but differs from it between 62 500 and 64 800 cm^{-1} both in substructure and in the presence in the optical spectrum of a more intense underlying near-continuum to the blue of 62 500 cm^{-1} that is absent from the REMPI spectrum. There are two differences between the optical and the REMPI experiments—the temperatures of the samples and the number of resonant photons. To determine which of these is responsible for the spectral difference, the room temperature REMPI spectrum was measured between 62 000 and 64 800 cm^{-1}. It is compared to the cold REMPI spectrum in Fig. 4. The spectra presented in Fig. 4 show that the warm sample has greater signal intensity in the underlying near continuum relative to that of the superimposed structured bands between 62 500 and 64 800 cm^{-1} than does the cold sample. The room temperature (3+1) REMPI spectrum is thus more similar, but not identical, to the optical spectrum: The underlying near-continuum of the optical spectrum is still more intense relative to the superimposed structured bands than in the room temperature REMPI spectrum.

An optical spectrum arises from the absorption of light by a molecule. A REMPI spectrum arises from only that fraction of the excited molecules that live long enough to absorb additional, ionization, photons. For short-lived states the results obtained by the two techniques may diverge.[39] To test for this phenomenon in the spectral region of acetone under discussion, the photoacoustic spectrum (PA) of acetone was also measured. Because a PA signal is generated by the energy released from a molecule on absorption, it is especially sensitive to nonradiative decay processes, hence to short-lived excited states. The PA spectrum of acetone between 62 000 and 64 800 cm^{-1} is presented in Fig. 4. We see that the signal from the underlying near-continuum is greatly enhanced in the PA spectrum of room temperature acetone relative to in the REMPI spectrum. In fact, the PA spectrum of acetone strongly resembles the optical spectrum. From these results we conclude, (1) that the spectrum of acetone around 63 000 cm^{-1} (7.8 eV) is composed of two transitions, one giving rise to the structured bands and the other to the diffuse background, (2) that the diffuse, quasicontinuous background that dominates the room temperature spectrum largely is due to a temperature-dependent state population or process, and (3) that the diffuse, quasicontinuous background arises from an excitation to a very short-lived excited state.

The warm and cold (3+1) REMPI and the PA spectra of acetone-d_6 were also measured. They are presented in Fig. 5. As for acetone we see that in the REMPI experiment warming the sample causes a great enhancement of the underlying continuum and that the continuum is further enhanced in the PA measurement relative to in the REMPI measurement. The apparent center of the enhanced absorption is 7.8 eV, similar to that observed for acetone. The positions of all bands were measured and are presented in Tables IV and V.

The interpretations of both the structured bands and the underlying continuum are not transparent. As noted above, the positions of the structured bands of the two isotopomers differ. More specifically, those observed in acetone-d_6 appear to originate 660 cm^{-1} to the blue of those observed in acetone with our selection of a ''local'' origin. Were they $3d$-Rydberg$\leftarrow\tilde{X}$ origins, as previously assigned,[2] they would be much closer. For comparison, the isotope blueshifts observed in the $3s$- and the three $3p$-Rydberg$\leftarrow\tilde{X}$ states are less than 30 cm^{-1}. By this criterion, none of the structured bands can be electronic origins. The dominant local separations between the structured bands are $\approx$325 and $\approx$1050 cm^{-1} in acetone and $\approx$295 and $\approx$830 cm^{-1} in acetone-d_6. These correspond to the dominant vibrational intervals observed in the $3p$-Rydberg$\leftarrow\tilde{X}$ transitions and assigned there as promotions of the CCC angle deformation and a methyl rocking

Downloaded¬29¬Jan¬2010¬to¬147.156.182.23.¬Redistribution¬subject¬to¬AIP¬license¬or¬copyright;¬see¬http://jcp.aip.org/jcp/copyright.jsp

TABLE IV. Experimental (3+1) REMPI spectrum of acetone.

Expt. wave length (nm)	(a)	Freq. (cm^{-1})	Dist. from X (cm^{-1})	Dist. from A (cm^{-1})	Dist. from B (cm^{-1})	Assignment (b)
482.72		62 148	−95			$X-12$
481.98	p	62 244	X			Local origin X
480.26		62 466	328−105			$X+8-12$
479.45	p	62 571	328			$X+8$
477.03	p	62 889	645			$X+8+8$ or
476.63	p	62 942	698			$X+16+16$
475.90		63 039				
475.50		63 092				
474.67	p	63 202	959			$X+8+8+8$ or
474.06	p	63 284	1040			$X+6$
472.94		63 434				
472.25		63 525	1373−91			$X+4-12$
471.58	p	63 616	1373			$X+4$
469.80		63 857				
469.31	p	63 924	1680			Several
467.37		64 188	1944			combinations
467.05		64 233				
462.87		64 814		−479		$A-8$
462.26		64 898		−395		$A-6$
460.58		65 135		−158		$A+8-8$
460.06		65 209		−84		$A-12$
459.47	sp	65 293		A		A origin
459.13		65 341				
457.21		65 615		322		$A+8$
456.35		65 738				
455.50	h	65 862			−83	$B-12$
455.31		65 889				
454.93	sp	65 944			B	B origin
453.06	h	66 216			272	$B+8-12$
452.49		66 300			356	$B+8$
448.53		66 884				
447.77		66 998			1054	$B+6$
446.25		67 227			1282	$B+5$ or 4
444.05		67 560			1615	$B+8+(4$ or $5)$
439.3		68 290			2346	$B+6+(4$ or $5)$
434.79	lp	68 999	C			C origin
432.6	lp	69 348	D			D origin

[a]p=peak, sp=strong peak, h=hot, lp=little peak.
[b]Numbers refer to vibrational modes. See Ref. 15 for assignments of vibrational modes.

modes[15] although the intensities of the subbands are greater in the present wavelength region than nearer the origins. We suggest, in contrast to our previous assignment,[15] that these bands are vibrational subbands of one or more of the $3p$-Rydberg$\leftarrow\tilde{X}$ transition, enhanced by interaction with another, energetically proximal, excited state. These observations and the electronic assignments of the structured and diffuse bands will be discussed below.

B. 65 000–67 000 cm^{-1} (8.0–8.3 eV) spectral region

The spectra of the two isotopomers in this wavelength region are similar, as shown in Fig. 2. Compared to the optical spectrum, the very intense band at 65 100 cm^{-1} and some of the higher energy substructure are the same but there is a second intense band in the REMPI spectrum that is absent from the optical spectrum. (The weak optical band that appears here is displaced approximately 40 cm^{-1} to the red of the strong REMPI band.) In this spectral region, warming the sample, Fig. 6, only induces a ''hot'' band to the red of the second intense peak in each isotopomer. The displacement of the hot band from the electronic origin, -82 cm^{-1} in acetone, -60 cm^{-1} in acetone-d_6 identifies it as the ground state a_2 torsion. As in the $3p$-Rydberg states, these two $3d$-Rydberg states are coupled by an a_2 torsion. They must, therefore, be either an A_1-A_2 or a B_1-B_2 pair in the C_{2v} symmetry group of acetone. However, since we have already demonstrated that neither of these transitions is A_2, the two electronic origins must be to B_1 and B_2 electronic states. The vibrational subbands of these transitions, given in columns 4 and 5 of Tables IV and V and assigned in column 6, arise from the same modes that were observed to be active in the $3s$- and $3p$-Rydberg$\leftarrow\tilde{X}$ transitions.[15] All group assignments will be discussed below.

VII. DISCUSSION

Here, we will discuss the ability of the theoretical method employed in this investigation to treat heavily mixed

Downloaded¬29¬Jan¬2010¬to¬147.156.182.23.¬Redistribution¬subject¬to¬AIP¬license¬or¬copyright;¬see¬http://jcp.aip.org/jcp/copyright.jsp

TABLE V. Experimental (3+1) REMPI spectrum of deuteroacetone.

Expt. wave length (nm)	(a)	Freq. (cm^{-1})	Dist. from X (cm^{-1})	Dist. from A (cm^{-1})	Dist. from B (cm^{-1})	Assignment (b)
481.25		62 337				
478.59		62 685	−219			$X-z$
477.70		62 801	−103			$X-y$
476.92	p	62 904	X			Local origin X
476.13		63 007	104			$X+y$
474.67		63 201	297			$X+8$
472.36		63 511	838−231			$X+6-z$
471.50		63 627	838−115			$X+6-y$
470.65	p	63 742	838			$X+6$
469.79		63 859	838+117			$X+6+y$
468.65		64 013	1110			$X+8+6$
466.40		64 323	1664−245			$X+6+6-z$
465.37		64 465	1664−103			$X+6+6-y$
464.62		64 568	1664			$X+6+6$
463.89		64 671	1664+103			$X+6+6+y$
461.41		65 018		−334		$A-16$
459.91		65 230		−122		$A-y$
459.05	sp	65 352		A		A origin
458.57		65 421		68		$A+12$
457.37		65 592				
457.08		65 634		281		$A+8$
456.03		65 785			−202	$B-z$
455.10	h	65 920			−67	$B-12$
454.64	sp	65 987			B	B origin
453.34		66 176		824		$A+6$
452.91		66 238			251	$B+8$
452.48		66 301				
449.90		66 681				
448.89		66 832			845	$B+6$
448.04		66 958			971	$B+4$
442.54		67 790			1804	$B+4+6$
436.09		68 793	C			C origin
432.59		69 350	D			D origin

[a]p=peak, sp=strong peak, h=hot, lp=little peak.
[b]Numbers refer to vibrational modes. y is ≈110 cm^{-1} and is twice ν_{12}. z is ≈230 cm^{-1} and is $\nu_{16}-\nu_{17}$. See Ref. 15 for assignments of vibrational modes.

excited configurations, specifically the $\pi\rightarrow\pi^*$ state of acetone. Central to this discussion is an analysis of the experimental assignments of the observed transitions of acetone and the correlations of the transition energies of the symmetry-assigned states with their computed values. In general, we expect the CASPT2 calculations to be accurate to better than 0.2 eV for all excited states that can be adequately treated by a perturbation method. Our result, that the $\pi\rightarrow\pi^*$ promotion energy changes when the σ,σ^* molecular orbital pair is included in the active space, suggests however that for states of $^1A_1$ symmetry, in particular the $^1A_1$ ($\pi\rightarrow\pi^*$) state, a second order perturbation method may not be accurate enough. Conversely, since the $\pi\rightarrow\pi^*$ state at the ground state geometry is well above the other states considered here, vertical transition energies should be calculated to the standard CASPT2 accuracy.

Most of these other states are Rydberg states, states in which one electron is promoted to an atomiclike orbital outside the molecular domain. Usually the equilibrium geometries of the ground and Rydberg states are similar and the lower Rydberg states do not interact strongly with each other or with excited valence states. Rydberg state calculations are, therefore, generally accurate although correlations with observed states are handicapped by the frequent experimental inability to detect all possible Rydberg states of a given type and to assign those that are observed. In acetone, four of the five lowest-lying states are Rydberg states—the $3s$- and three $3p$-Rydberg states. These and the $n_y\rightarrow\pi^*$ valence state have been previously assigned. Not only are the calculated and experimental energies of these states in agreement, Table III, but, as noted above, so are their calculated and relative experimental intensities. The two highest energy states observed here, at 8.55 and 8.60 eV are assigned as transitions from the ground to two of the $4p$-Rydberg states on the basis of their quantum defects of 0.56 and 0.48. These states were not considered in the theoretical study.

Between the $3p$- and $4p$-Rydberg states lie the $4s$, $3d$, and possibly the $\pi\rightarrow\pi^*$ and $\sigma\rightarrow\pi^*$ valence states. At the ground state equilibrium geometry the latter are very high in energy. Because their equilibrium geometries are greatly displaced from the ground state geometry, their spectra are predicted to possess long Franck–Condon envelopes leading to

Downloaded¬29¬Jan¬2010¬to¬147.156.182.23.¬Redistribution¬subject¬to¬AIP¬license¬or¬copyright;¬see¬http://jcp.aip.org/jcp/copyright.jsp

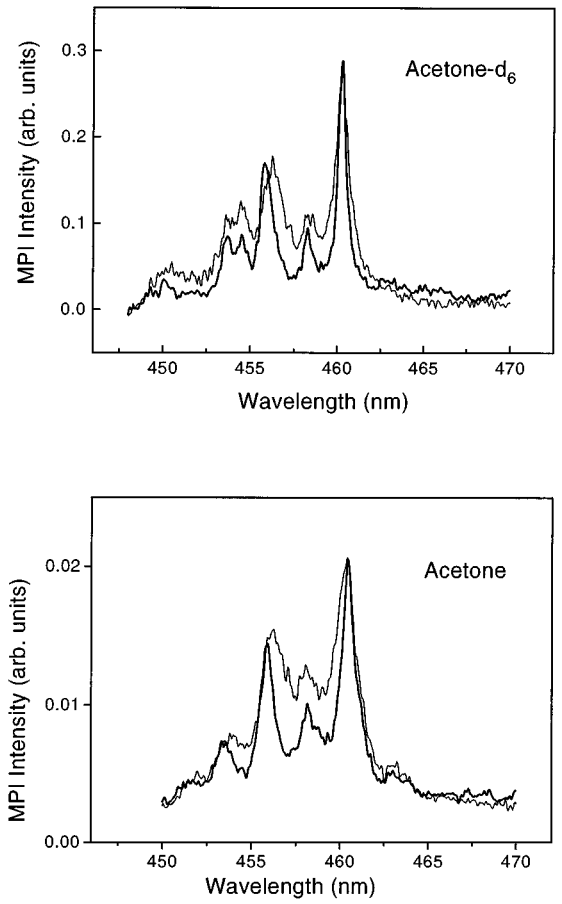

FIG. 6. (3+1)REMPI spectra of cold (heavy lines) and "warm" (light lines) acetone and acetone-d_6.

the peak intensity. As this is not observed for the strong transitions occurring around 8 eV, the valence transitions will not be considered initially. All five $3d$-Rydberg states are calculated to lie between 7.9 and 8.2 eV (the EOM-CC study of Gwaltney and Bartlett[20] places them somewhat higher, between 8.0 and 8.5 eV, but this is most likely due to the use of a smaller basis set in their study, which does not include explicit Rydberg functions). The $4s$-Rydberg state was not calculated, but is expected to lie here also. Thus transitions to six Rydberg states are possible around 8 eV. Of the $3d$ states, the transition to the A_1 state is calculated to be intense, that to the lower energy B_2 state about 1/7th as intense, and to the other three states, weaker or forbidden. Only two transitions are observed here. One very strong transition is observed around 8.09 eV in the optical spectrum and this and one other, at 8.19 eV, are observed in the REMPI spectrum. Because their vibrational substructures correspond to those previously observed for the $3s$- and $3p$-Rydberg$\leftarrow\tilde{X}$ transitions and they are observed by REMPI spectroscopy, both transitions are assigned as transitions to Rydberg states. The question can now be asked, to which Rydberg states. Because the 1-photon intensity of the $A_1\leftarrow\tilde{X}$ $3d$-Rydberg transition is calculated to be much larger than that of any of the other $3d$-Rydberg transitions, one's first inclination would be to assign the very intense origin observed in both the REMPI and optical spectra at 8.08 eV to the A_1 $3d$-Rydberg state. This cannot be however, because such an assignment disagrees with the experimental assignment of the two REMPI-observed Rydberg origins as a B_1-B_2 pair. Thus we reject this assignment for the optically observed transition and ask, instead, to which B_1 and B_2 Rydberg states do the experimentally-observed origins correspond. There is only one possible B_1 Rydberg state—the B_1 $3d$-Rydberg state. It is calculated to give rise to a weak optical transition at 8.20 eV. There are three possible B_2 states, two $3d$- and the $4s$-Rydberg states. While the transition energy to the $4s$-Rydberg state was not calculated here, from the quantum defect of the transition to the $3s$-Rydberg state we estimate it to be around 8.2 eV. The two $3d$-Rydberg states are calculated to lie at 8.04 and 8.18 eV. Because the separation between the two experimentally observed states is 0.12 eV, and there is only one B_1-B_2 pair with a calculated energy separation around 0.1 eV, we assign the lower energy experimentally observed transitions as from the ground to the B_2 $3d$-Rydberg state and the upper to the B_1 $3d$-Rydberg state. We note that the calculated (8.04 and 8.20 eV) and experimental (8.08 and 8.16 eV) transition energies are in agreement. We also note that the calculated intensities are not in agreement with this assignment—most notibly the A_1 $3d$-Rydberg state, which is calculated to be very intense, is not observed. We will return to this point below.

The identities of the very short-lived diffuse absorption around 7.8 eV and the structured transitions superimposed on it will now be considered. The center of the diffuse band is at approximately the same energy in the two isotopomers, which suggests that this is an electronic origin. The only transition calculated to originate at this energy is to the $^1A_1$ $3d$-Rydberg state. We tentatively give this assignment to the diffuse transition. By contrast, the dissimilar energies of the structured transitions in the two isotopomers indicate that they are unlikely to represent a discrete electronic transition. We suggest that they are vibrational subbands of one of the lower-energy $3p$-Rydberg$\leftarrow\tilde{X}$ transitions that have been enhanced by an energetically proximal transition. It is not possible to identify which $3p$-Rydberg state because it was not possible to determine the symmetry of the structured bands and because the observed local origin—$3p$-Rydberg separation is approximated in energy by several combinations built on either the A_1 or B_2 $3p$-Rydberg band. It is, however, possible to estimate the location of the perturbing transition. The local origin in acetone is 7.71 eV, hence the perturber must be below this. Because the local origin in deuteroacetone is much higher in energy than in acetone we assume that the observed transition corresponds to one more quanta of the unknown upper state vibrational mode in deuteroacetone than in acetone. From the observed local origin in deuteroacetone, 7.80 eV, and the frequency of its largest vibrational interval, 2250 cm^{-1} in the ground state (0.28 eV), a lower limit for the perturbing state is estimated to be 7.52 eV. We conclude that the unobserved state that is perturbing one of the $3p$-Rydberg$\leftarrow\tilde{X}$ transitions in acetone lies between 7.5 and 7.7 eV. We note that this is approximately where the

Downloaded¬29¬Jan¬2010¬to¬147.156.182.23.¬Redistribution¬subject¬to¬AIP¬license¬or¬copyright;¬see¬http://jcp.aip.org/jcp/copyright.jsp

A_1 valence and A_1 $3p$ Rydberg potential curves are calculated to cross.

The experimental spectrum has now been assigned to the extent permitted by the data. Several anomalies in the spectrum have been observed, the most prominent of which are that the band assigned as the A_1 $3d$-Rydberg origin is exceedingly diffuse and increases in intensity when the molecule is ''warm'' and that high vibrational overtones of one of the $3p$-Rydberg origins are active. When these results are compared with the theoretical calculations one other anomaly immediately stands out: the exceedingly intense band assigned as the transition to the B_2 $3d$-Rydberg state is observed to be much more intense than the band assigned as the transition to the A_1 $3d$-Rydberg state, which is calculated to be the strongest. We also note that no direct evidence of the $\pi\rightarrow\pi^*$ valence-excited state has been detected.

To unify the theoretical results and the experimental anomalies we propose that all the anomalies are due to interactions of the different Rydberg states (or transitions) with a short-lived $\pi\rightarrow\pi^*$ state located approximately where it has been calculated in this investigation. A proposed exceedingly short lifetime of the $\pi\rightarrow\pi^*$ state broadens the transition to this state to the extent that it appear only as a diffuse background beneath the experimentally resolved transitions to the Rydberg states. Strong coupling between the $\pi\rightarrow\pi^*$ state and the A_1 $3d$-Rydberg state shortens the lifetime of the latter, hence broadens its observed spectrum. Heating the molecule may, in fact, reduce the coupling strength, lengthen the lifetime of the Rydberg state, and hence intensify the transition as detected by the REMPI technique. Weaker coupling between the A_1 valence and the A_1 $3d$-Rydberg states restricts their interaction to close to where the two potential curves cross. It is this interaction that induced intensity in the of higher vibrational quanta of the $3p$-Rydberg state. And, lastly, indirect coupling between the $\pi\rightarrow\pi^*$ and the B_2 $3d$-Rydberg state is proposed to cause the observed intensification of the latter state.

VII. SUMMARY AND CONCLUSIONS

Results have been presented from a combined *ab initio* and experimental investigation of the main features of the electronic spectrum of acetone. In the theoretical calculation, vertical transition energies were calculated from the ground to the $n_y\rightarrow\pi^*$, $\pi\rightarrow\pi^*$, $\sigma\rightarrow\pi^*$, and the $n=3$ Rydberg states. In addition, the $^1A_1$ energy surfaces were studied as functions of the CO bond length. Because of the shape and position of the $\pi\rightarrow\pi^*$ potential surface, the $^1A_1$ $3p$ and $3d$ states were found to be heavily perturbed by the $\pi\rightarrow\pi^*$ state. In the experimental investigation, the $(3+1)$ REMPI and PA spectra of acetone, observed transitions and those observed by optical spectroscopies were assigned on internal criteria. The experimental and theoretical results were then compared and conclusions drawn.

The calculated vertical transition energies to the $n_y\rightarrow\pi^*$ and all Rydberg states that were observed were found to be in agreement with their experimental values. This includes the $3s$-, all three $3p$- and the A_1, B_1, and B_2 $3d$-Rydberg states. By contrast, there is little agreement between the calculated and experimental relative intensities of the A_1 and B_2 $3d$-Rydberg transitions. In addition, anomalously intense high vibrational overtone bands of one of the $3d$-Rydberg transitions were observed. These results were interpreted as experimental signs of the strong perturbation of the $3p$- and $3d$-Rydberg states by the $\pi\rightarrow\pi^*$ state found in the theoretical calculation. The elusive $^1A_1$ $\pi\rightarrow\pi^*$ state is inferred to be similar to that calculated.

ACKNOWLEDGMENTS

The research reported in this communication has been supported by a grant from the Swedish Natural Science Research Council (NFR) and by DGICYT Project No. PB94-0986 of Spain.

[1] E. E. Barnes and W. T. Simpson, J. Chem. Phys. **39**, 670 (1963).
[2] R. H. Huebner, R. J. Celotta, S. R. Mielczarek, and C. E. Kuyatt J. Chem. Phys. **59**, 5434 (1973).
[3] M. B. Robin, in *Higher Excited States of Polyatomic Molecules*, (Academic, New York, 1974) Vol. 2.
[4] W. M. St. John III, R. C. Estler, and J. P. Doering, J. Chem. Phys. **61**, 763 (1974).
[5] P. Brint, K. Wittel, P. Hochmann, W. S. Felps, and S. P. McGlynn, J. Am. Chem. Soc. **98**, 7980 (1976).
[6] K. N. Walzl, C. F. Koerting, and A. Kuppermann, J. Chem. Phys. **87**, 3796 (1987).
[7] R. McDiarmid and A. Sabljić, J. Chem. Phys. **89**, 6086 (1988).
[8] A. Gedanken and R. McDiarmid, J. Chem. Phys. **92**, 3237 (1990).
[9] J. G. Philis, J. M. Berman, and L. Goodman, Chem. Phys. Lett. **167**, 16 (1990).
[10] R. McDiarmid, J. Chem. Phys. **95**, 1530 (1991).
[11] S. N. Thakur, D. Guo, T. Kundu, and L. Goodman, Chem. Phys. Lett. **199**, 335 (1992).
[12] T. Kundu, S. N. Thakur, and L. Goodman, J. Chem. Phys. **97**, 5410 (1992).
[13] K. Furuya, S. Katsumata, and K. Kimura, J. Electron Spectrosc. Relat. Phenom. **62**, 237 (1993).
[14] J. G. Philis and L. Goodman, J. Chem. Phys. **98**, 3795 (1993).
[15] X. Xing, R. McDiarmid, J. G. Philis, and L. Goodman, J. Chem. Phys. **99**, 7565 (1993).
[16] H. Zuckermann, Y. Haas, M. Drabbels, J. Heinze, L. Meerts, J. Reuss, and J. v. Bladel, Chem. Phys. **163**, 193 (1992).
[17] M. Merchán and B. O. Roos, Theor. Chim. Acta **92**, 227 (1995).
[18] B. Hess, P. J. Bruna, R. J. Buenker, and S. D. Peyerimhoff, Chem. Phys. **18**, 267 (1976).
[19] V. Galasso, J. Chem. Phys. **92**, 2495 (1990).
[20] S. R. Gwaltney and R. J. Bartlett, Chem. Phys. Lett. **241**, 26 (1995).
[21] N. L. Allinger, M. P. Cava, D. C. De Jongh, C. R. Johnson, N. A. Lebel, and C. L. Stevens, *Organic Chemistry* (Worth, New York, 1971).
[22] J. M. Hollas, *Modern Spectroscopy* (Wiley, Chichester, 1987).
[23] M. Hachey, P. J. Bruna, and F. Grein, J. Chem. Soc. Faraday Trans. **90**, 683 (1994).
[24] M. R. J. Hachey, P. J. Bruna, and F. Grein, J. Phys. Chem. **99**, 8050 (1995).
[25] M. Baba, I. Hanazaki, and U. Nagashima, J. Chem. Phys. **82**, 3938 (1985).
[26] D. J. Donaldson, G. A. Gaines, and V. Vaida, J. Phys. Chem. **92**, 2766 (1988).
[27] H. Zuckermann, B. Schmitz, and Y. Haas, J. Phys. Chem. **93**, 4083 (1989).
[28] B. O. Roos, in *Advances in Chemical Physics; Ab Initio Methods in Quantum Chemistry—II*, edited by K. P. Lawley (Wiley, Chichester, 1987), Chap. 69, p. 399.
[29] K. Andersson, P.-Å. Malmqvist, B. O. Roos, A. J. Sadlej, and K. Wolinski, J. Phys. Chem. **94**, 5483 (1990).
[30] K. Andersson, P.-Å. Malmqvist, and B. O. Roos, J. Chem. Phys. **96**, 1218 (1992).
[31] K. Andersson and B. O. Roos, in *Modern Electron Structure Theory*, edited by R. Yarkony (World Scientific, New York, 1994), Vol. 1.

Downloaded¬29¬Jan¬2010¬to¬147.156.182.23.¬Redistribution¬subject¬to¬AIP¬license¬or¬copyright;¬see¬http://jcp.aip.org/jcp/copyright.jsp

[32] B. O. Roos, M. P. Fülscher, Per-Åke Malmqvist, M. Merchán, and L. Serrano-Andrés, in *Quantum Mechanical Electronic Structure Calculations with Chemical Accuracy*, Dordrecht, edited by S. R. Langhoff (Kluwer Academic, Amsterdam, 1995).
[33] R. Nelson and L. Pierce, J. Mol. Spectrosc. **18**, 344 (1965).
[34] P.-O. Widmark, P.-Å. Malmqvist, and B. O. Roos, Theor. Chim. Acta **77**, 291 (1990).
[35] B. O. Roos, M. Merchán, R. McDiarmid, and X. Xing, J. Am. Chem. Soc. **116**, 5927 (1994).
[36] L. Serrano-Andrés, M. Merchán, I. Nebot-Gil, R. Lindh, and B. O. Roos, J. Chem. Phys. **98**, 3151 (1993).
[37] P. Å. Malmqvist and B. O. Roos, Chem. Phys. Lett. **155**, 189 (1989).
[38] K. Andersson, M. P. Fülscher, G. Karlström, R. Lindh, P.-Å. Malmqvist, J. Olsen, B. O. Roos, A. J. Sadlej, M. R. A. Blomberg, P. E. M. Siegbahn, V. Kellö, J. Noga, M. Urban, and P.-O. Widmark, *MOLCAS Version 3*. Dept. of Theor. Chem., Chem. Center, Univ. of Lund, P.O.B. 124, S-221 00 Lund, Sweden, Lund, (1994).
[39] X. Xing, A. Gedanken, A.-H. Sheybani, and R. McDiarmid, J. Phys. Chem. **98**, 8302 (1994).
[40] R. R. Pappalardo, M. Reguero, M. A. Robb, and M. Frish, Chem. Phys. Lett. **212**, 12 (1993).
[41] J. Gao, J. Am. Chem. Soc. **116**, 9324 (1994).
[42] D. M. Friedrich, J. Chem. Phys. **75**, 3258 (1981).
[43] J. D. Swalen and C. C. Costain, J. Chem. Phys. **31**, 1562 (1959).

Downloaded¬29¬Jan¬2010¬to¬147.156.182.23.¬Redistribution¬subject¬to¬AIP¬license¬or¬copyright;¬see¬http://jcp.aip.org/jcp/copyright.jsp